Geomatics Research Australasia

A WGS84–AHD PROFILE OVER THE DARLING FAULT, WESTERN AUSTRALIA

O.J. Friedlieb [1]
W.E. Featherstone [1]
M.C. Dentith [2]

1. School of Surveying and Land Information
Curtin University of Technology
Perth, WESTERN AUSTRALIA

2. Department of Geology and Geophysics
The University of Western Australia
Perth, WESTERN AUSTRALIA

ABSTRACT

The Darling Fault near Perth in Western Australia causes a steep geoid gradient of approximately 100mm/km. Existing gravimetric geoid models cannot currently recover this rapidly varying geoid undulation with sufficient accuracy so as to allow the accurate determination of Australian Height Datum (AHD) heights using the Global Positioning System (GPS). As such, the geometrical approach to determine the separation between the AHD and World Geodetic System 1984 (WGS84) ellipsoid is expected to offer improved GPS height determination in this region. A network of 45 carrier-phase GPS baselines, made at 14 first-order AHD benchmarks at ~3km intervals along a 30km profile across the Darling Fault near Perth, was observed in order to test this hypothesis. Several GPS network adjustment strategies were implemented which constrained existing height information in different ways. Due to the poor knowledge of the position of the geoid in this region, the most precise network adjustment used only one fixed ellipsoidal height and all other known stations were held fixed in latitude and longitude only. When the geometrical approach was compared with the results of existing gravimetric geoid solutions, it offers a superior means of determining heights from GPS. However, the geometrical method only satisfies third-order specifications in 5 of the 12 cases tested in this region of the Darling Fault.

1. INTRODUCTION

Global Positioning System (GPS) observations in conjunction with optical levelling on the Australian Height Datum (AHD) enable a direct estimation of the position of the geoid at discrete points. This concept is not new and has been described by, for example, Gilliland (1986), Mitchell (1988), Dickson and Zahra (1992) and Collier and Croft (1995), among others. The geometrical difference between the geoid and the World Geodetic System 1984 (WGS84) ellipsoid (ΔN_{WGS84}) is realised through:

$$\Delta N_{WGS84} = \Delta h_{WGS84} - \Delta H_{AHD} \quad , \tag{1}$$

where Δh_{WGS84} is the WGS84 ellipsoidal height difference provided by relative GPS measurements, and ΔH_{AHD} is the height difference provided by optical levelling [and surface gravity measurements if it is to truly be an orthometric height; see Holloway (1988) and Torge (1991)].

This is referred to as the geometrical approach to geoid modelling and only requires a knowledge of the Earth's gravity field along the levelling route instead of over a large area surrounding each computation point, as is the case with the gravimetric method. The principal advantage of using the geometrical approach is that the majority of any common errors in GPS heights, orthometric heights, or both, are reduced when using equation (1). However, the proficiency with which the geometrical approach can be used to determine AHD heights is ultimately limited by: the precision of the GPS-derived WGS84 ellipsoidal heights; the definition of, and undulations in, the AHD, which is also assumed to be coincident with the geoid; and, the type of interpolation surface used.

In practice, the geometrical approach is applied in the following way: Given GPS heights at AHD benchmarks that surround a survey area, and GPS heights at points within this survey area, the AHD heights of these inner points can be derived by interpolating the GPS-derived geoid heights from the surrounding control stations. The interpolation surface used to model the geometrical geoid is generally a plane or low-order polynomial, each generated by least squares techniques if redundancy exists. A higher order polynomial surface should be used with extreme caution as this can often create spurious geoid undulations, especially in areas of sparse AHD control.

Accurate geometrical modelling of the short-wavelength undulations between the AHD and WGS84 also requires that the control stations are sufficiently dense. Gilliland (1986) indicates that linear interpolation over distances of approximately 25km can result in errors exceeding 4mm/km, if disturbances exist in the local gravity field. This situation occurs around Perth, Western Australia, where GPS height determination has proven problematic due to perturbations of the gravity field associated with a major geological structure called the Darling Fault. As such, the

current AUSGEOID93 national gravimetric geoid model (Steed and Holtznagel, 1994) rarely produces AHD heights that are acceptable to the Western Australian Department of Land Administration. Therefore, the geometrical approach has been used to provide a profile of the short-wavelength AHD-WGS84 undulations across the Darling Fault near Perth, and thus determine whether the geometrical approach offers a superior alternative with which to achieve GPS height determination in this region.

The Darling Fault profile is referred to the WGS84 ellipsoid, and was derived from a network of 45 relative GPS baselines co-located with high-order spirit-levelled AHD benchmarks. It should, therefore, be noted that this profile specifically provides a measure of the separation between the AHD and WGS84, as opposed to the separation between the classically defined geoid (W = constant) and WGS84. This is due to the fact that the geoid, AHD and mean sea-level around Australia are not coincident (Mather *et al*., 1976; Featherstone, 1995) and that the AHD is not a true orthometric height system because observed gravity data were not used in its definition (Roelse *et al*., 1971; Holloway, 1988).

As such, the geometrical method was expected to offer an improvement in GPS-derived AHD heights over the existing AUSGEOID93 gravimetric geoid model. It was also expected to provide improvements since it is of a higher spatial resolution, and thus samples higher frequency undulations in the AHD with respect to WGS84. The data collected also allow for a comparison between gravimetric and geometrical methods for the subsequent determination of AHD heights from GPS in the Perth region of the Darling Fault. The three resulting sets of GPS-derived AHD heights have been analysed using GPS control at AHD benchmarks in the profile, and were also compared to third-order spirit-levelling misclosure tolerances.

2. THE PERTURBATION OF THE GRAVITY FIELD DUE TO THE DARLING FAULT

The Darling Fault is one of the largest geological structures in Australia and is a significant structure on a world scale. The fault extends for more than 1,000km, running approximately north-south a few tens of kilometres inland from the west coast of Western Australia.

The approximate position of the fault can be easily determined due to an associated change in topography. To the west of the fault is the coastal plane, whilst to the east are gentle hills reaching a few hundred metres in height (Figure 1). The contrasting topography is the result of the fault juxtaposing two very different types of rock. To the east of the fault are rocks, some of which are more than three billion years old, that belong to a geological entity referred to as the Yilgarn Craton. The majority of these rocks are various types of granite, and being crystalline, are relatively resistant to erosion. In contrast, to the west of the fault are various types of

sedimentary rocks, such as sandstones and shales, which were deposited in the Perth Basin. These rocks are comparatively young, being about 130 to 430 million years old. The sedimentary rocks are much more easily eroded than those of the Yilgarn Craton resulting in a scarp, close to the position of the fault.

Geological studies of the Darling Fault and its surrounds have shown the Darling Fault to be a comparatively young and narrow structure located in an older, wider zone of deformation, called the proto-Darling Fault (Blight *et al*., 1981). The proto-Darling Fault is associated with crustal deformation extending over a zone up to 30km wide, along the western margin of the Yilgarn Craton. This feature was in existence more than 2.6 billion years ago (Compston *et al*., 1986). The Darling Fault, however, is associated with some of the youngest events in this zone of deformation.

The fault resulted from oblique extension where the rocks of the Perth Basin in the west has been displaced downwards with respect to the Yilgarn Craton in the east. Seismic reflection data indicate that the fault is near vertical and the displacement on the fault in excess of 10km is likely (Dentith *et al*., 1993).

Figure 1. A representative profile of the gravity anomaly and topography across the Darling Fault near Perth, Western Australia

The rocks either side of the Darling Fault have a distinct contrast in physical properties, most notably their bulk densities. The sediments in the Perth Basin have a density of about 2,000kgm^{-3}, whilst those in the Yilgarn Craton are between about 2,500kgm^{-3} and 3,000kgm^{-3}. The large displacement on the Darling Fault means that a very large thickness of low and high density rock types are juxtaposed which results in a significant perturbation of the gravity field. As illustrated in Figure 1, in the vicinity of the Darling Fault profile, there is a gravity anomaly with an amplitude in excess of 100mgal and a wavelength of about 50km.

The presence of the gravity field associated with the Darling Fault also creates a steep geoid gradient of approximately 100mm/km. Due to the inability of AUSGEOID93 to accurately model short-wavelength disturbances in the gravity field, such as the effects of the Darling Fault, it rarely produces GPS-derived AHD heights which meet the third-order tolerance in the Perth region. Therefore, it was expected that the geometrical method could provide a superior alternative to AHD height determination from GPS in the vicinity of the Darling Fault.

3. THE GPS SURVEY AND NETWORK ADJUSTMENT

The project upon which this account is based (Friedlieb, 1995) utilised a network of GPS baselines measured to 14 first-order AHD benchmarks mostly at 3km intervals along a ~30km profile over the Darling Scarp. The GPS network comprised a total of 45 baselines, observed between July and August 1995, and which is shown in Figure 2. Dual-frequency, carrier-phase GPS data were recorded for approximately two hours per baseline, using two *Trimble 4000SSE Geodetic System Surveyor* receivers. Double difference processing was performed using all the observables present to produce integer fixed baseline vectors and their corresponding variance-covariance matrices.

Figure 2. The geometry of the network of GPS baselines used to define the WGS84-AHD profile across the Darling Fault, Western Australia.

3.1 Effect of the Horizontal Datum on the Network Adjustment

A minimally constrained adjustment was applied to the GPS network by fixing only Caversham R371 in latitude, longitude and height. This is both a second-order terrestrial geodetic control station of the Australian Geodetic Datum 1984 (AGD84) and GPS-positioned station of the Geocentric Datum of Australia (GDA).

The three-dimensional WGS84 co-ordinates of Caversham R371 were estimated by transforming its AGD84 and AHD values using Higgins's (1987) parameters and AUSGEOID93 (Steed and Holtznagel, 1994), respectively. These co-ordinates deviate by approximately 0.5m from the GDA co-ordinates, which have been observed directly by GPS. This difference is due to local horizontal distortions between the AGD84 and GDA networks and errors in AUSGEOID93.

Firstly, the three-dimensional GDA co-ordinates of Caversham R371 were held fixed in the minimally constrained adjustment. The standardised residuals verified the internal consistency of the GPS network, based on the geometric connections between all relative baseline vectors. The 45 GPS baselines gave a variance of unit weight as 0.94 with 142 degrees of freedom in the minimally constrained solution. The precision of baselines at the 95% confidence interval varied between 6mm/km to 0.5mm/km for baselines from 3km to 30km in length, respectively.

The compatibility of the existing geodetic control with the GDA was then assessed by comparing the GPS-derived co-ordinates of BA28 and SAWY to their transformed WGS84 values given on Western Australian Standard Survey Mark summary sheets. The systematic vector misclosures are shown in Table 1, which are compliant with the deviation between the GDA and transformed WGS84 co-ordinates observed at Caversham R371.

Table 1. The vector misclosure due to datum differences in geodetic control when GDA co-ordinates instead of transformed WGS84 co-ordinates are held fixed at R371.

Station	*Misclosure Easting (m)*	*Misclosure Northing (m)*	*Misclosure Distance (m)*	*Misclosure Bearing*
R371	-0.540	-0.129	0.555	256° 33' 52.1150"
BA28	-0.547	-0.174	0.574	252° 21' 15.1170"
SAWY	-0.478	-0.161	0.504	251° 23' 07.5880"

The vector offsets in Table 1 translate to a 9.1" rotation and a 1:36,000 scale error between R371 and BA28, and a 5.4" rotation and 1:58,000 scale error between R371 and SAWY. Therefore, the co-ordinate recoveries of this minimally constrained adjustment do not endorse the integration of 'pure' GDA and transformed WGS84 co-ordinates for the control of GPS networks. This also highlights the importance of

readjusting existing geodetic infrastructure onto the GDA and the use of projective transformation parameters from the AGD84 to WGS84 that also account for any local network distortions (Featherstone, 1997).

The minimally constrained adjustment was repeated using only the transformed WGS84 co-ordinates of R371 to define the datum. The compatibility of the geodetic control was again analysed by comparing the GPS-derived co-ordinates of BA28 and SAWY to their transformed WGS84 values, published on Western Australian Standard Survey Mark summary sheets. The misclosures are presented in Table 2.

Table 2. The misclosure when only transformed WGS84 co-ordinates are used as fixed geodetic control in the minimally constrained network adjustment.

Station	*Misclosure Easting (m)*	*Misclosure Northing (m)*	*Misclosure Distance (m)*	*Misclosure Bearing*
R371	0.000	0.000	0.000	0° 00’ 00.0000”
BA28	-0.006	-0.044	0.044	187° 45’ 54.5970”
SAWY	0.062	-0.031	0.078	127° 09’ 52.1090”

The shifts in Table 2 translate into a –0.1” rotation and 1:250,000 scale error between R371 and BA28, and a 3.0” rotation and 1:352,000 scale error between R371 and SAWY. This magnitude of these errors over baselines of 10km to 25km exceeds the claimed accuracy of the AGD84, which endorses the likelihood of local network distortions being present. However, these residual misclosures may also represent systematic errors in the GPS network, which is less likely given its precision. In addition, Higgins’s (1987) conformal transformation parameters cannot represent any local distortions in the AGD84, even in this relatively small area.

The misclosures summarised in Tables 1 and 2, reinforce the need to use a single, self-consistent horizontal datum when constraining local GPS networks. The transformed WGS84 co-ordinates and the GDA co-ordinates are not compatible in this instance, and thus should not be mixed until AGD data are readjusted onto the GDA. This also indicates that if the GDA is implemented by a transformation from the AGD, a projective approach should be used as this can also account for any local distortions between these datums.

3.2 The Effect of *a priori* Geoid Heights on the Network Adjustment

The objective of a constrained network adjustment is to obtain an optimum fit to the local geodetic datum. Therefore, when additional control stations are held fixed, the precision of the resulting co-ordinates in a GPS network will generally be degraded with respect to the results of the minimally constrained adjustment. This is primarily

due to distortions in the existing geodetic network that are revealed when using more precise GPS observations (cf. Lambert, 1982). However, the effect of the geoid on any constrained network adjustment must also be considered, as has been identified by Collins (1989), Zilkoski and Hothem (1989) and Sideris (1990), for example.

For instance, a local GPS network is often tied to a terrestrial geodetic control station, whose WGS84 co-ordinates have been realised using a transformation. As local heights refer to an approximation of the geoid, a geoid model must also be used to realise the WGS84 ellipsoidal heights of the control stations. Therefore, any errors in the geoid model will directly affect the co-ordinates derived from the network adjustment, if more than one transformed WGS84 height is held fixed.

Therefore, the WGS84 co-ordinates of the Darling Scarp GPS-AHD profile have been computed using a variety of adjustment approaches in order to estimate the effect of the geoid gradient in this extreme case. Four of the different network adjustment strategies tested are outlined in Table 3. This procedure also included the derivation and assessment of local horizontal co-ordinate transformation parameters, which can account for the inconsistency between the GPS observations and the local geodetic control (cf. Olliver, 1996).

Table 3. The four constrained network adjustments compared in order to quantify the effect of the geoid on the accuracy of the resulting co-ordinates.

Station	*Phase #1*	*Phase #2* †	*Phase #3*	*Phase #4* ‡
R371	Constrained 3D	Constrained 3D	Constrained 3D	Constrained 3D
BA28	Constrained 2D	Constrained 2D	Constrained 3D	Constrained 3D
SAWY	Constrained 2D	Constrained 2D	Constrained 3D	Constrained 3D

† The adjusted heights in Phase #2 are obtained via the derivation of only a local scale factor.

‡ The adjusted heights in Phase #4 are obtained via the derivation of a local scale factor and three rotation parameters.

A comparison of the results of the four phases of constrained network adjustment (Table 3) with the minimally constrained adjustment are shown in Figures 3 and 5. Figures 4 and 6 show the 95% vertical error at stations along the profile for each adjustment strategy. The 95% confidence vertical error at each station, derived from the Phase #2 and Phase #4 adjustments is approximately 30mm, which is commensurate with the precision attained by Brunner and Tregonning (1994) and Hajela (1990).

A visual analysis of these graphs suggests that the Phase #2 adjustment, where a local scale factor was derived, provides the optimum solution both in terms of WGS84 ellipsoidal heights and vertical errors. The determination of a local scale factor and three rotation parameters in the Phase #4 adjustment further reduces the WGS84 height

errors, as estimated by the adjustment. However, the difference between the Phase #4 and minimally constrained adjustments (Figure 5) shows that by fixing more than one WGS84 ellipsoidal height distorts the derived WGS84 co-ordinates by 0.36m over the 30km distance (12mm/km) and should thus not be used.

Figure 3: The differences between WGS84 heights derived from the Phase #1 and Phase #2 adjustments with respect to the minimally constrained solution.

Figure 4: The 95% vertical error estimates for WGS84 heights derived from the Phase #1 and Phase #2 network adjustments.

Figure 5: The differences between WGS84 heights derived from the Phase #3 and Phase #4 adjustments with respect to the minimally constrained solution.

Figure 6: The 95% vertical error estimates for WGS84 heights derived from the Phase #3 and Phase #4 network adjustments.

Overall, the results shown in Figures 3 to 6 indicate that the Phase #2 adjustment provides the smallest error ellipses, whilst also avoiding a systematic distortion in the WGS84 ellipsoidal heights due to an imprecise knowledge of the geoid gradient. However, it should be noted that when using the geometrical approach to GPS height determination, the tilt between the Phase #2 and Phase #4 adjustments can often be

accounted for, and thus eliminated, as part of the interpolation process. Nevertheless, such a conceptually imprecise approach should be avoided wherever possible.

4. RESULTS AND ANALYSIS

The hypothesis tested in this study was that the geometrically derived WGS84-AHD separation, when used in conjunction with linear interpolation over short distances (~3km), would improve upon the gravimetric geoid for GPS height determination in the Perth region of the Darling Fault.

It was also expected that the geometrical method would produce AHD heights from GPS which satisfy third-order spirit-levelling misclosure tolerances in Western Australia (12√km mm). Significantly, compliance with third-order levelling standards on the AHD would indicate that GPS, in conjunction with the local WGS84-AHD geometrical model, offers a more accurate replacement for AUSGEOID93 in the Perth region of the Darling Fault.

4.1 Realisation of the Geometrical WGS84-AHD Profile

The geometrical difference between the WGS84 ellipsoidal and AHD heights was resolved using equation (1) at the series of AHD benchmarks across the Darling Fault. The resulting profile of 14 geometrical WGS84-AHD heights exhibits a steep east-west gradient. Least squares regression was used to estimate the linear gradient as 3.8m over the 35km traverse, corresponding to 108mm/km.

Table 3. High-frequency variations in the WGS84-AHD profile across the Darling Fault.

Leg	*Baseline Length (m)*	*WGS84-AHD Difference (m)*	*WGS84-AHD Gradient (mm/km)*
UB48-MWS316	3285.895	0.175	53.257
MWS316-MWS323	3010.768	0.477	158.431
MWS323-UB54	3029.034	0.146	48.200
UB54-UB55	2073.626	0.263	126.831
UB55-HZ656	1954.872	0.283	144.766
HZ656-F397A	3384.851	0.521	153.921
F397A-F396A	2591.792	0.342	131.955
F396A-F395A	2806.751	0.376	133.963
F395A-F394	1496.022	-0.222	-148.394
F394-F393B	3000.775	0.684	227.941
F393B-F392	3112.575	0.307	98.632
F392-F391	3526.951	0.263	74.569
F391-F391A	1532.200	-0.393	-256.494

However, the gravity field is also relatively disturbed, as exhibited by the short-wavelength undulations. The relative slope was, therefore, also determined for each of the 13 legs along the spirit-levelled traverse. Table 3 presents the high frequency variations that exist in the geometric technique which are considerably different to the average gradient of the profile, thus indicating the presence of high frequency variations.

4.2 Comparison of AHD Height Recovery from GPS

Recall that the combination of GPS and spirit-levelling data specifically models the WGS84-AHD separation, rather than the classical WGS84-ellipsoid-geoid separation, and thus absorbs any systematic GPS errors, spirit-levelling errors, or both. This approach can also account for the fact that the AHD uses normal orthometric heights instead of true orthometric heights (Holloway, 1988), and that the AHD is tied to tide-gauge measurements of sea-level and is thus not necessarily an equipotential surface of the Earth's gravity field (Mather *et al*., 1976; Featherstone, 1995).

However, the presence of gross and random errors in the GPS or AHD control data should not be totally disregarded. Levelling errors or disturbances in sections of the AHD can remain undetected in this technique of geometrical geoid modelling. As such, both AHD and GPS errors are inevitably incorporated, which propagate directly into the interpolation and thus degrade the comparisons with spirit-levelled AHD stations. Nevertheless, this approach does give AHD heights that are fully compatible with existing AHD heights, and thus eliminates the biases between the AHD and AUSGEOID93.

In this investigation, three specific geoid modelling alternatives were considered:

1. Linear interpolation of the geometrical WGS84-AHD heights;
2. AUSGEOID93 rigorously computed gravimetric geoid heights, kindly provided by the Australian Surveying and Land Information Group (AUSLIG); and,
3. AUSGEOID93 gravimetric geoid heights bi-cubically interpolated from the standard 10' by 10' grid using the *Winter* software, also supplied by AUSLIG.

In each case, the GPS-derived AHD height was compared with the spirit-levelled AHD height, and the most accurate method is deemed to be the one that provides the smallest discrepancy.

The differences between AHD heights, derived from GPS using the geometric and gravimetric co-ordinate transformations, and spirit-levelled AHD heights are presented in Figure 7. From the 14 benchmarks occupied with GPS, only 12 have been used in the analysis because the geometrical method has been based on the two nearest benchmarks, thus precluding a comparison for benchmarks UB48 and F391A.

Figure 7. Height discrepancies when using the linearly interpolated geometrical WGS84-AHD values (solid line), AUSGEOID93 interpolated values (broken line) and AUSGEOID93 rigorously computed values (dotted line), as compared to spirit-levelled AHD heights.

The geometrical co-ordinate transformation is clearly superior to the gravimetric co-ordinate transformation, as evidenced by the smaller overall misclosures in Figure 7. However, the misclosures for all three methods are anomalous at 6.29km and 23.63km, for example. These misclosures are significantly greater than the ellipsoidal height error implied by the GPS network adjustment (±0.03m), which suggests one of two causes:

1. The AHD data used to compare these geoid modelling techniques are in error; or,
2. The short wavelength geoid undulations cannot be accurately modelled by linear interpolation.

The former explanation is a more likely scenario because the levelling traverse was originally conducted in 1961, and the benchmarks may have settled or been disturbed during urban development. However, independent checks on the height of these benchmarks by repeat levelling and cross-checks against witness marks have validated the integrity of these marks. The exact cause of these anomalous results is, therefore, still under investigation.

4.3 Comparison with Third-order Levelling Tolerances

Next, the AHD heights derived from each of the three methods at benchmarks along the Darling Fault profile were compared to the third-order spirit-levelling misclosure tolerance in Western Australia (12√km mm), and are shown in Figures 8, 9 and 10.

The discrepancies between the three approaches and the control AHD heights have been plotted with the cumulative baseline length being used to calculate the misclosure tolerance.

In Figure 8, linear interpolation of the WGS84-AHD values provided AHD heights which satisfy third-order criteria in five of the 12 cases. Therefore, this technique does not consistently recover third-order standards. This may be due to errors in the AHD and GPS control data, or short-wavelength variations in the gravity field (Table 3) which can not be accurately modelled by linear interpolation alone. Nevertheless, this geometrical approach is superior to using AUSGEOID93 in both its rigorous and interpolated forms: the AHD heights derived from GPS using the rigorously computed (Figure 9) and interpolated (Figure 10) AUSGEOID93 values lie outside third-order specifications in all but one case.

It is also evident from Figure 8 that the geometrical approach can provide AHD heights which satisfy third-order standards, in cases where the relative geoid slope is regular along the Darling Scarp profile (cf. Table 3). The geometrical approach also provides a significant improvement over the AUSGEOID93 gravimetric geoid model over shorter baselines. This is due to the increased resolution of the geometrical approach, as provided by the detailed GPS and spirit-levelling data over the Darling Fault.

Figure 8. Difference between levelled AHD and GPS-derived AHD heights compared to third-order standards, using the geometrical method

There is broad agreement between the results obtained from the AUSGEOID93 rigorously computed *N* values (Figure 9), and the AUSGEOID93 interpolated *N* values (Figure 10). This is to be expected, since the geoid heights for each data set are derived from the OSU91A global geopotential model and the Australian Geological Survey Organisation's (AGSO) digital gravity data-base (Steed and Holtznagel, 1994).

Figure 9. Difference between levelled AHD and GPS-derived AHD heights compared to third-order standards, using AUSGEOID93 rigorously computed *N* values

Figure 10. Difference between levelled AHD and GPS-derived AHD heights compared to third-order standards, using AUSGEOID93 interpolated *N* values**.**

However, some larger differences (eg. ~0.2m at benchmark MWS323 or 6.29km) are due to interpolation errors as *Winter* uses a 10' by 10' grid which does not agree with the rigorous solution. Therefore, it is recommended that AUSGEOID93 should use a higher resolution grid interval in regions of steep geoid gradients so as to reduce these interpolation errors.

In addition to the graphical presentations of the results, Table 4 provides a summary of the numerical analysis carried out for each approach to GPS height determination in the Perth region of the Darling Fault. This is similar to the way in which results are presented in other geoid studies and allows a direct comparison.

Table 4: Summary of the AHD height differences over the Darling Fault profile (units in metres)

Statistic	*Geometrical Interpolation*	*AUSGEOID93 Rigorous*	*AUSGEOID93 Interpolated*
max.	0.354	0.274	0.341
min.	-0.002	0.008	-0.036
mean	0.034	0.148	0.148
std. dev.	±0.198	±0.128	±0.165
% third-order	42 %	8 %	8 %

Of most concern is that the geometrical method gives the largest overall standard deviation of the differences, whereas it proves the most suitable for the determination of AHD heights from GPS (according to third-order tolerances). Therefore, if a geoid model is to be used for subsequent AHD height determination, validations based only on simple statistical differences can be misleading. Note also, however, that the mean differences decrease for the geometrical technique, which illustrates that it does indeed remove the biases between the gravimetric geoid solution and the AHD.

5. CONCLUSIONS

As expected, the AUSGEOID93 gravimetric geoid model, when applied to GPS heights in both its rigorous and bi-cubically interpolated forms, does not satisfy third-order spirit-levelling criteria in the Perth region of the Darling Fault. Conversely, GPS heights, when used in conjunction with the linearly interpolated model of WGS84-AHD separation, provides AHD heights that are superior to those obtained from AUSGEOID93 in both forms. However, the geometrical approach still does not produce AHD heights which consistently satisfy third-order ($12\sqrt{}$km mm) spirit-levelling misclosure limits in Western Australia.

The linear geometrical method still proves deficient in cases where high frequency undulations exist between data points defining the WGS84-AHD separation, even over the short distances used in this study. However, the quality of the spirit-levelled AHD control data could be a contributing factor as to why the geometrical interpolation did not consistently attain third-order specifications.

To conclude, the geometrical method, whilst conceptually more appropriate, has not provided a satisfactory solution to the problem of GPS height determination near Perth. Nevertheless, it is demonstrably superior to the gravimetric AUSGEOID93 and satisfies third-order tolerances in approximately half of the cases tested in this study. Future modelling of the AHD-WGS84 separation near Perth will use a combination of geometric and gravimetric techniques.

ACKNOWLEDGEMENTS

All the authors wish to thank: Ian Barrie, of the Western Australian Department of Land Administration (DOLA), for prompting this investigation; Jim Steed, of the Australian Surveying an Land Information Group (AUSLIG), for providing the AUSGEOID93 geoid model in both its forms; and, the staff of DOLA, especially Jim Payne, for providing the spirit-levelling data and information as to its quality. This research was funded as part of Australian Research Council grants A49331318 and A44391011.

REFERENCES

Blight, D.F., W. Compston and S.A. Wilde, 1981. The Logue Brook granite: Age and significance of deformation zones along the Darling Scarp, *Geological Survey of Western Australia, Annual Report 1980*, 72-80.

Brunner, F.K. and P. Tregonning, 1994. Investigation of height repeatability from GPS measurements. *Australian Journal of Geodesy, Photogrammetry and Surveying*, 60: 33-48.

Compston, W., I.S. Williams and M.T. McCulloch, 1986. Contrasting U-Pb and model Sm-Nd ages for the Archaean Logue Brook granite, *Australian Journal of Earth Sciences*, 33: 193-200.

Collins, J. (1989) Fundamentals of GPS baseline and height determinations. *Journal of Surveying Engineering*, 115(2): 223-235.

Collier, P.A. and M.J. Croft, 1995. Heights from GPS in an engineering environment. *Surveying Australia*, 17(3): 27-38.

Dentith, M.C., I. Bruner, A. Long, M.F. Middleton and J. Scott, 1993. Structure of the eastern margin of the Perth Basin, Western Australia, *Exploration Geophysics*, 24: 455-462.

Dickson, G. and C. Zahra, 1992. NSW-Vic high precision GPS network modelling the geoid, *Proceedings of the National Conference on GPS Surveying*, Sydney, NSW, 123-141.

Featherstone, W.E., 1995. On the use of Australian geodetic datums in gravity field determination. *Geomatics Research Australasia*, 62: 17-36.

Featherstone, W.E., 1997. A comparison of existing transformation models and parameters in Australia, *Cartography*, 26(1): 13-25.

Friedlieb, O.J., 1995. Geometrical determination of a local geoid model for Perth using GPS, *BSurv Honours Dissertation*, School of Surveying and Land Information, Curtin University of Technology, Perth, Western Australia.

Gilliland, J.R., 1986. Heights and GPS. *The Australian Surveyor*, 33(4): 277-283.

Higgins, M., 1987 Transformation from WGS84 to AGD84: an interim solution. *Internal Report*, Department of Geographic Information, University of Queensland.

Hajela, D., 1990. Obtaining centimetre-precision heights by GPS observations over small areas. *GPS World*, 1(1): 55-59.

Lambert, B.P., 1981. Australian geodetic coordinates keeping up with the times. *The Australian Surveyor*, 30(8): 491-504.

Manning, J. and B. Harvey, 1994. Status of the Australian geocentric datum. *The Australian Surveyor*, 39(1): 28-33.

Mather, R.S., Rizos, C., Hirsch, B. and Barlow, B.C., 1976. An Australian gravity data bank for sea surface topography determinations (AUSGAD76), *UNISURV G-25*, School of Surveying, The University of New South Wales, 54-84.

Mitchell, H.L., 1988. GPS heighting in Australia: an introduction. *The Australian Surveyor*, 34(1): 5-10.

Olliver, J.G., 1996. A simple adjustment procedure for local GPS networks. *The Australian Surveyor*, 41(4): 288-293.

Roelse, A., H.W. Granger and J.W. Graham, 1971. The adjustment of the Australian levelling survey 1970-71. *Technical Report 12*, Division of National Mapping, Canberra, Australian Capital Territory.

Sideris, M.G., 1990. The role of the geoid in one-, two-, and three-dimensional network adjustments. *Canadian Institute of Surveying and Mapping Journal*, 44(1): 9-18.

Steed, J. and S. Holtznagel, 1994. AHD heights from GPS using AUSGEOID93. *The Australian Surveyor*, 39(1), 21-27.

Torge, W., 1991. *Geodesy* (second edition). Walter de Gruyter, Berlin.

Zilkoski, D.B. and L.D. Hothem, 1989. GPS satellite surveys and vertical control. *Journal of Surveying Engineering*, 115(2): 262-281.

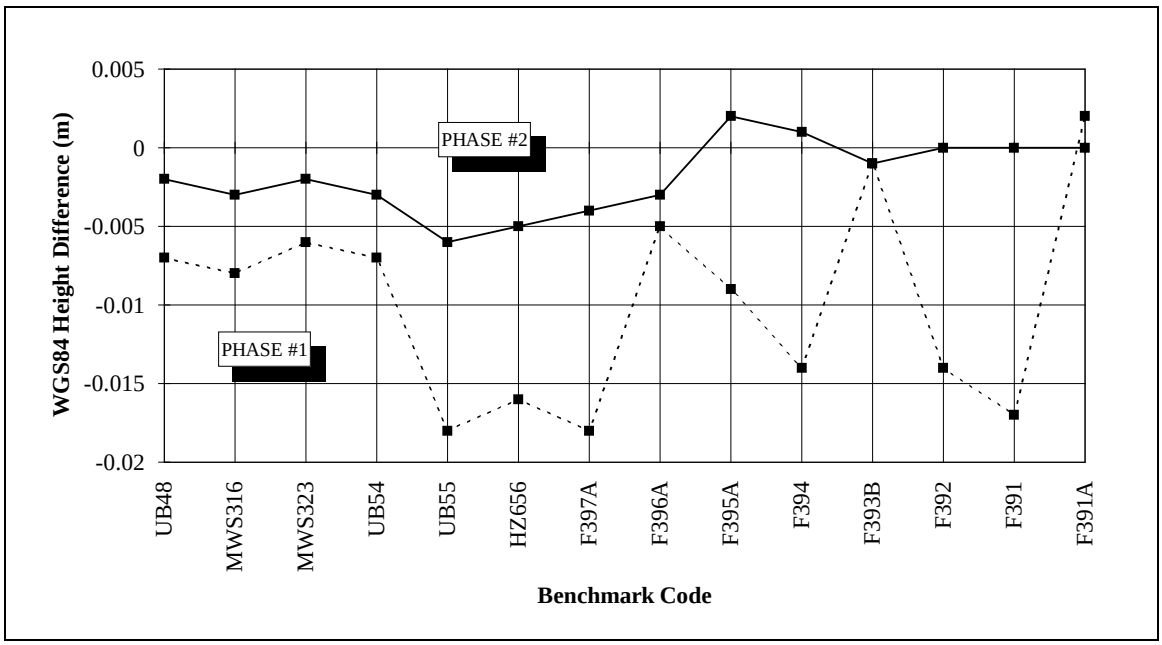

Figure 4: Difference between WGS84 heights derived from the Phase #1 and Phase #2 adjustments with respect to the minimum constraint solution

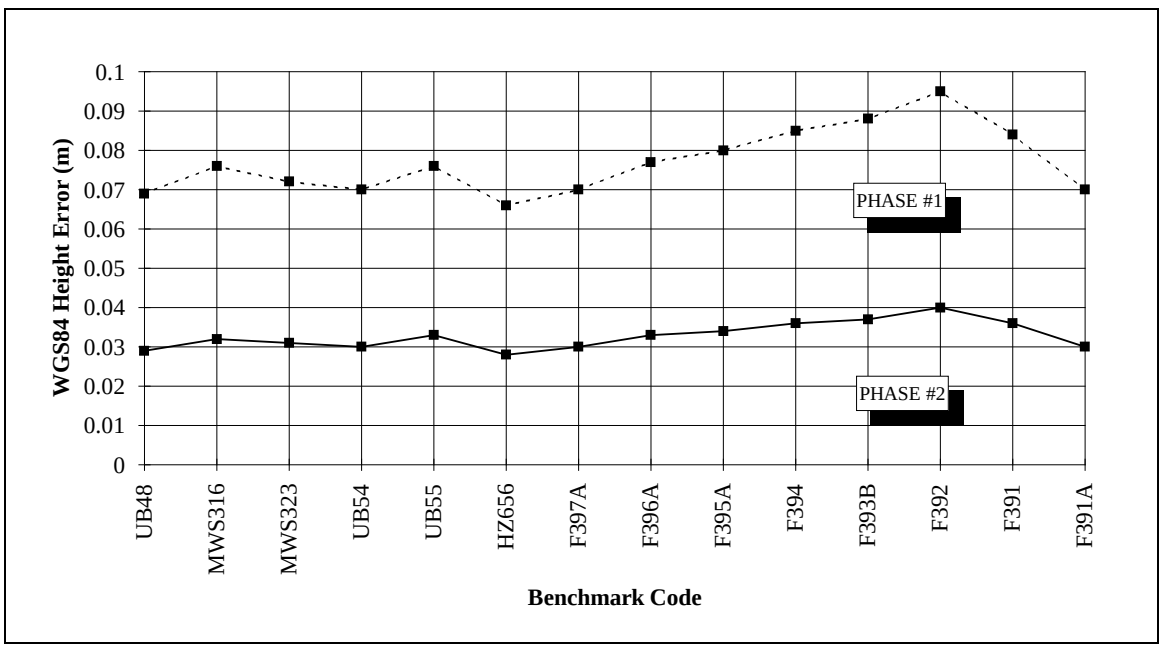

Figure 5: The 95 percent vertical error for WGS84 heights from the Phase #1 and Phase #2 network adjustments

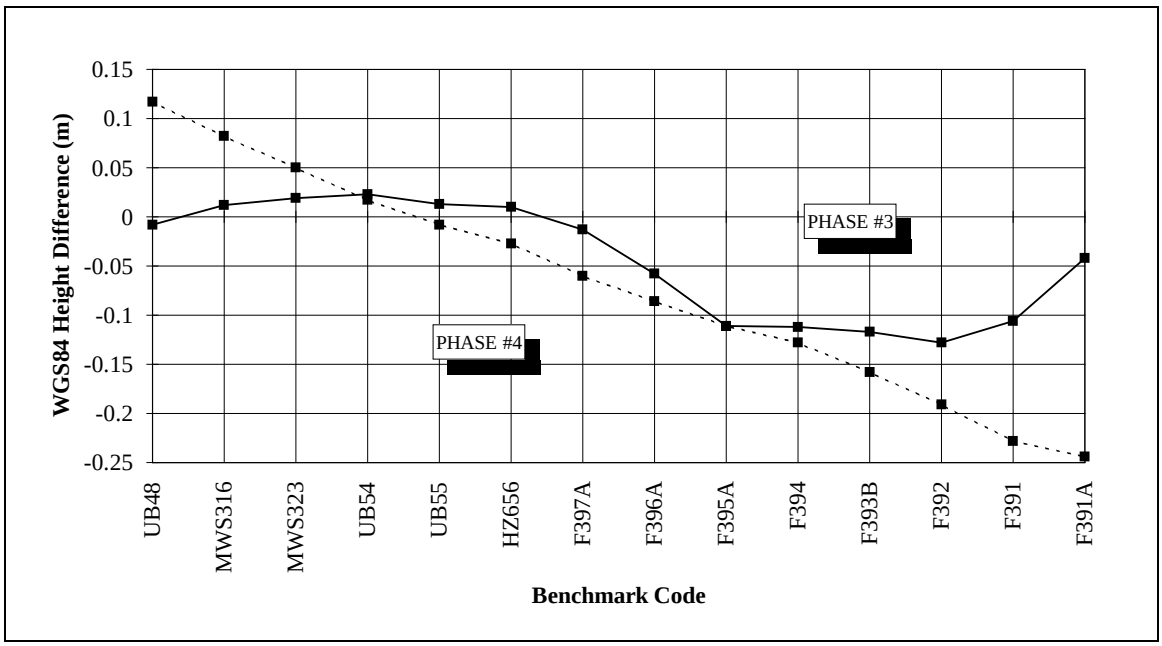

Figure 6: Difference between WGS84 heights derived from the Phase #3 and Phase #4 adjustments with respect to the minimum constraint solution

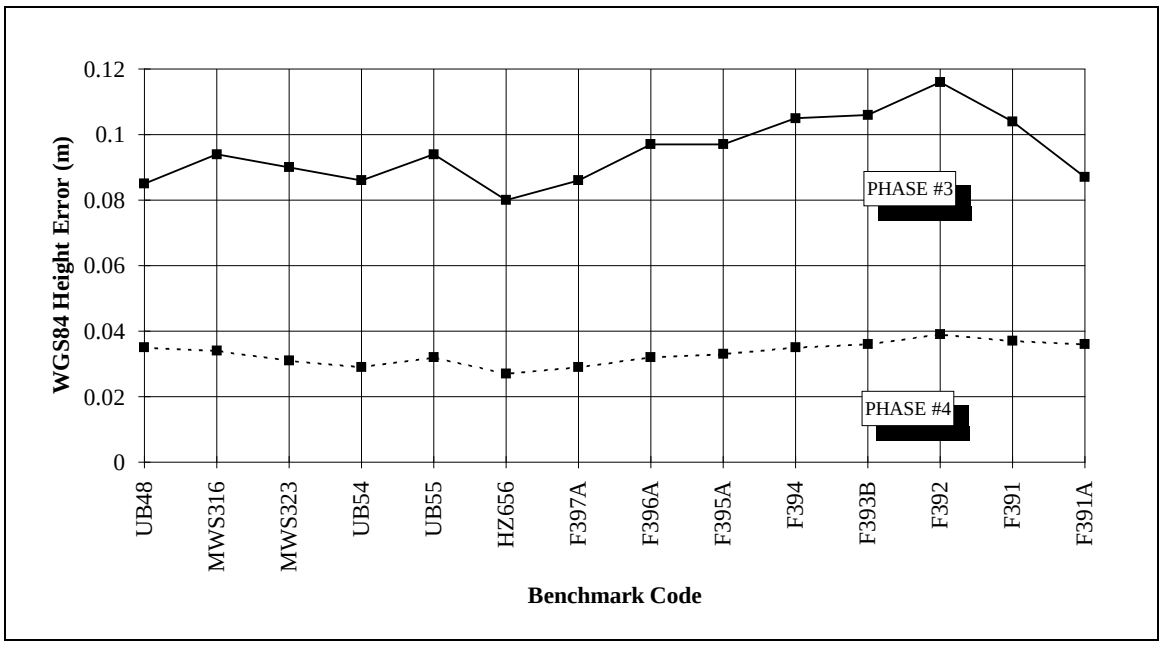

Figure 7: The 95 percent vertical error for WGS84 heights from the Phase #3 and Phase #4 network adjustments

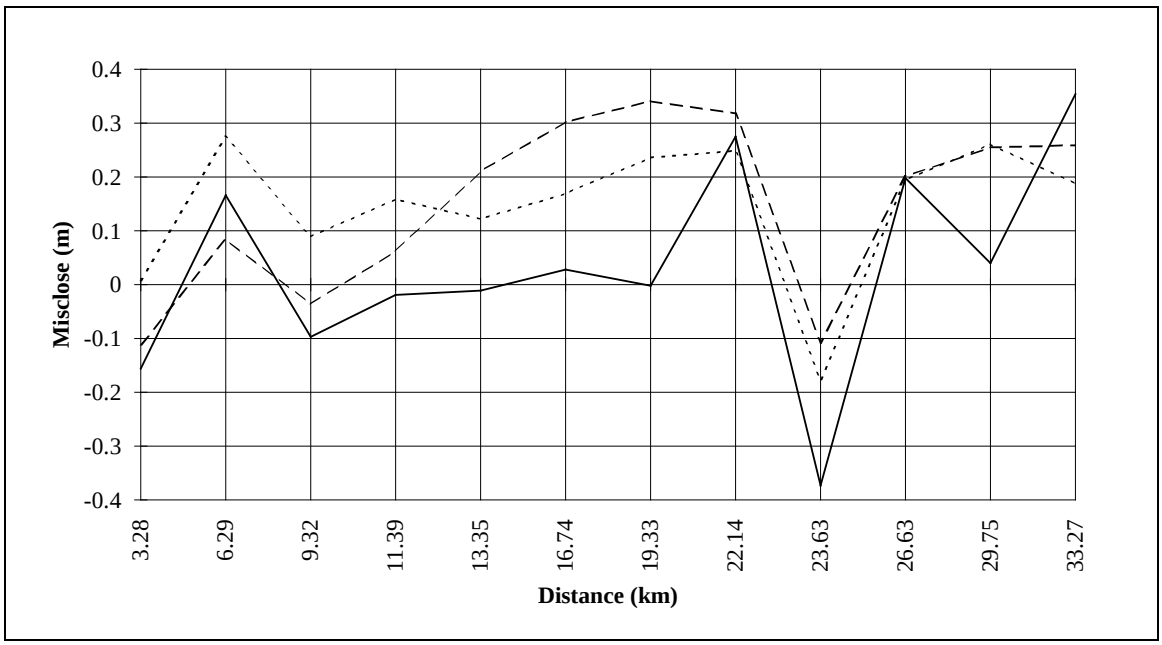

FIGURE 8.3: Discrepancies in the geometrically interpolated N values (solid line), AUSGEOID93 interpolated N values (broken line), and AUSGEOID93 rigorous N values (dotted line) in comparison to GPS and spirit-levelling data

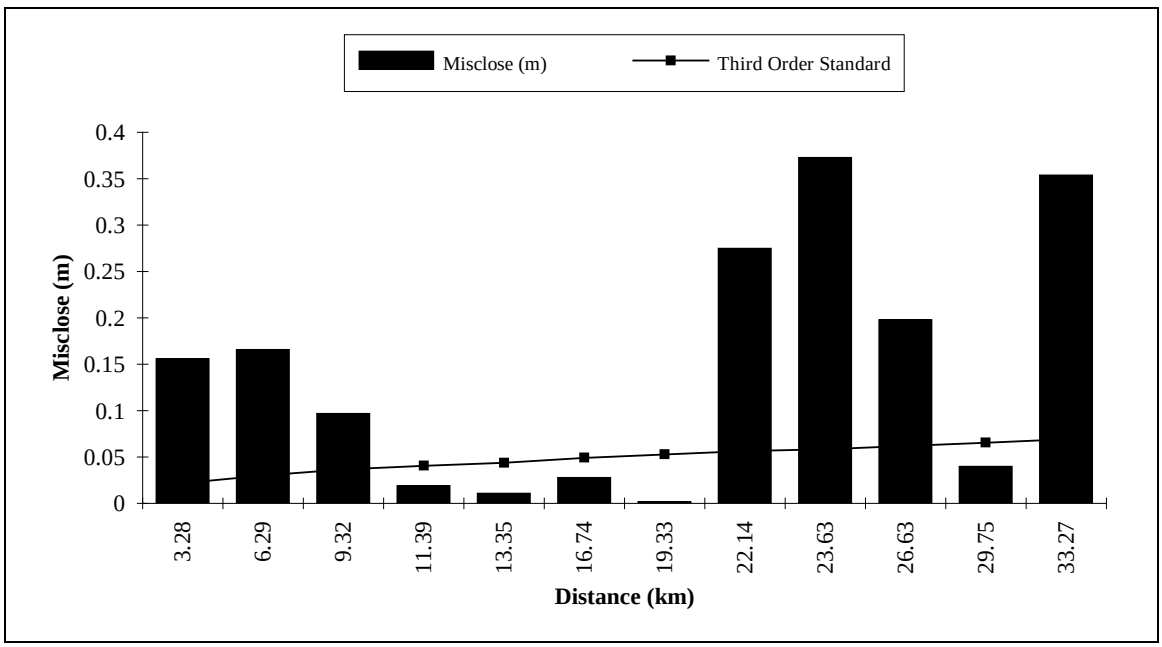

FIGURE Difference in AHD minus GPS-derived AHD heights compared to third order standards, using geometrically interpolated N values

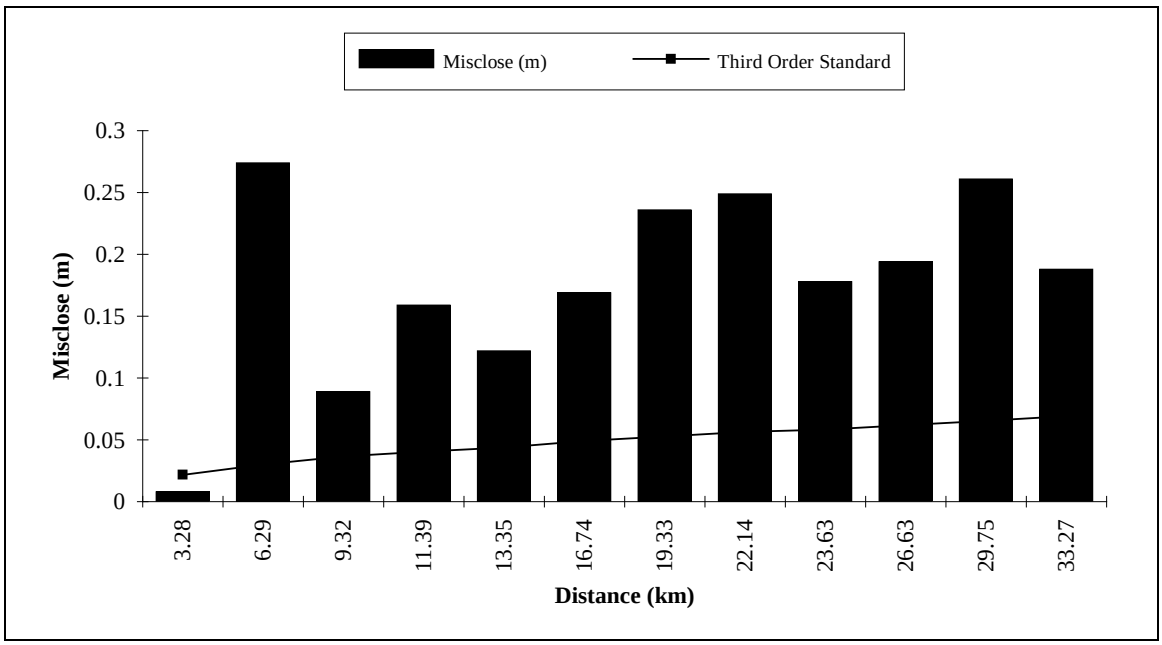

FIGURE Difference in AHD minus GPS-derived AHD heights compared to third order standards, using AUSGEOID93 rigorously computed N values

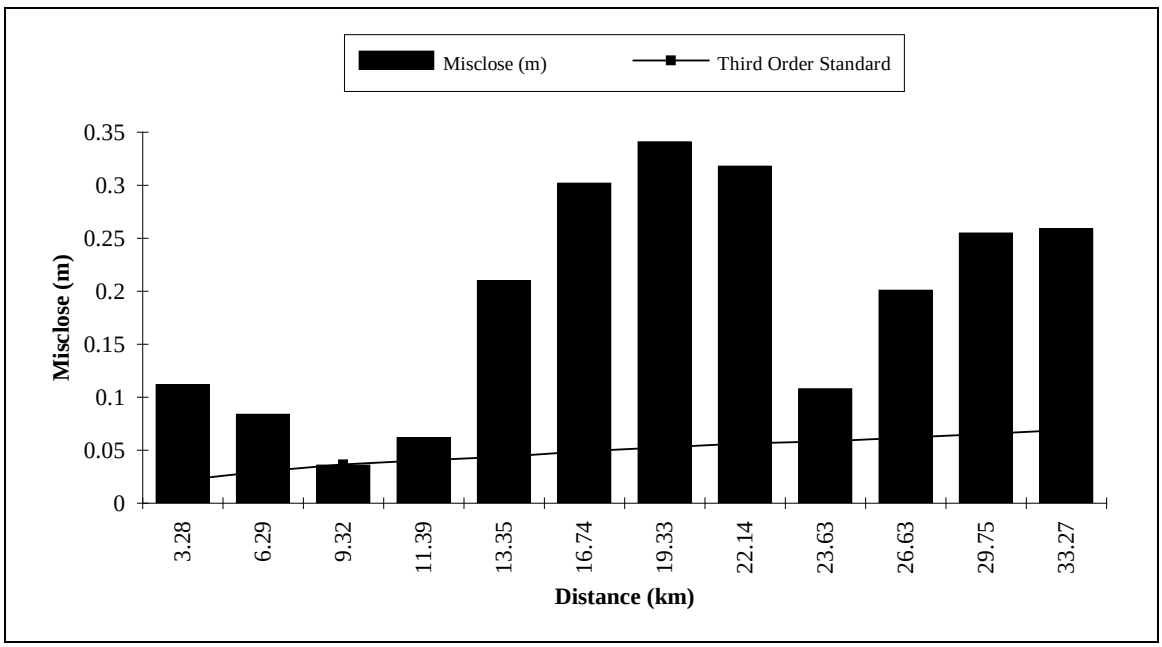

FIGURE Difference in AHD minus GPS-derived AHD heights compared to third order standards, using AUSGEOID93 interpolated N values